Adipocyte-Specific Overexpression of FOXC2 Prevents Diet-Induced Increases in Intramuscular Fatty Acyl CoA and Insulin Resistance

Jason K. Kim,[1] Hyo-Jeong Kim,[1] So-Young Park,[1] Anna Cederberg,[2] Rickard Westergren,[2] Daniel Nilsson,[2] Takamasa Higashimori,[1] You-Ree Cho,[1] Zhen-Xiang Liu,[1] Jianying Dong,[1] Gary W. Cline,[1] Sven Enerback,[2] and Gerald I. Shulman[1,3,4]

Insulin resistance plays a major role in the development of type 2 diabetes and may be causally associated with increased intracellular fat content. Transgenic mice with adipocyte-specific overexpression of FOXC2 (forkhead transcription factor) have been generated and shown to be protected against diet-induced obesity and glucose intolerance. To understand the underlying mechanism, we examined the effects of chronic high-fat feeding on tissue-specific insulin action and glucose metabolism in the FOXC2 transgenic (Tg) mice. Whole-body fat mass were significantly reduced in the FOXC2 Tg mice fed normal diet or high-fat diet compared with the wild-type mice. Diet-induced insulin resistance in skeletal muscle of the wild-type mice was associated with defects in insulin signaling and significant increases in intramuscular fatty acyl CoA levels. In contrast, FOXC2 Tg mice were completely protected from diet-induced insulin resistance and intramuscular accumulation of fatty acyl CoA. High-fat feeding also blunted insulin-mediated suppression of hepatic glucose production in the wild-type mice, whereas FOXC2 Tg mice were protected from diet-induced hepatic insulin resistance. These findings demonstrate an important role of adipocyte-expressed FOXC2 on whole-body glucose metabolism and further suggest FOXC2 as a novel therapeutic target for the treatment of insulin resistance and type 2 diabetes. *Diabetes* 54:1657–1663, 2005

From the [1]Department of Internal Medicine, Yale University School of Medicine, New Haven, Connecticut; the [2]Department of Medical Biochemistry, Medical Genetics, Goteborg University, Goteborg, Sweden; the [3]Department of Cellular and Molecular Physiology, Yale University School of Medicine, New Haven, Connecticut; and the [4]Howard Hughes Medical Institute, Yale University School of Medicine, New Haven, Connecticut.

Address correspondence and reprint requests to Prof. Jason K. Kim, Yale University School of Medicine, Department of Internal Medicine, Section of Endocrinology and Metabolism, The Anlyan Center, S269C, 300 Cedar St., P.O. Box 208020, New Haven, CT 06520-8020. E-mail: jason.k.kim@yale.edu.

Received for publication 20 May 2004 and accepted in revised form 16 March 2005.

IKK-β, inhibitor of κB kinase-β; IRS, insulin receptor substrate; PI, phosphatidylinositol; PKC, protein kinase C; PPAR, perixisome proliferator–activated receptor; PTP, protein-tyrosine phosphatase.

Insulin resistance is a major characteristic and early requisite event in the development of type 2 diabetes, which is reaching epidemic proportions in the world (1). Although the mechanism of insulin resistance is unknown, alteration in adipocyte metabolism may precede and cause insulin resistance in skeletal muscle and liver (2–7). Numerous factors implicated in this process include altered expression of adipocyte-derived factors (i.e., resistin, adiponectin, leptin, interleukin-6, tumor necrosis factor-α) (8–13) and fatty acids (14–16). Previous studies (8–13) have demonstrated increased adipocyte expression of resistin, interleukin-6, and tumor necrosis factor-α or reduced expression of adiponectin and leptin to promote insulin resistance. Other studies (17–20) have shown a strong inverse relationship between intracellular fat content and insulin sensitivity in both animal models and humans. Increases in circulating fatty acid levels and increasing fatty acid delivery into skeletal muscle or liver by tissue-specific overexpression of lipoprotein lipase caused insulin resistance (18). In contrast, decreasing fatty acid uptake into skeletal muscle with deletion of fatty acid transporters (i.e., FAT/CD36 and FATP1) improved insulin sensitivity and protected mice from developing diet-induced insulin resistance (21,22). Thus, it is clear that alteration in adipocyte metabolism plays an important role in the pathogenesis of insulin resistance.

Human winged helix/forkhead transcription factor gene (FOXC2) has been shown to be expressed in adipocytes and plays a key regulatory role in adipocyte metabolism (23). To determine the metabolic role of FOXC2, we have recently generated mice with adipocyte-specific overexpression of FOXC2, and these mice were shown to be protected against diet-induced obesity and glucose intolerance (23). These effects were associated with increased expression of genes associated with adipocyte metabolism (e.g., uncoupling protein-1) and enhanced sensitivity of the β-adrenergic/cAMP/protein kinase A pathway in the FOXC2 transgenic (FOXC2 Tg) mice (23). Increased number and size of adipocyte mitochondria were also evident in the FOXC2 Tg mice, overall indicating enhanced adipocyte metabolism in the Tg mice (23). These changes in adipocyte metabolism resulted in less adiposity and normal glucose tolerance following high-fat diet compared with the wild-type mice (23). To determine the effects of

FOXC2 overexpression on tissue-specific glucose metabolism, we performed a hyperinsulinemic-euglycemic clamp experiment and assessed insulin action and insulin signaling in the FOXC2 Tg mice following 3 weeks of high-fat diet. Our results demonstrate that overexpression of FOXC2 prevented diet-induced insulin resistance in skeletal muscle and liver, and this was associated with reduced accumulation of intracellular fatty acyl CoA levels in skeletal muscle.

RESEARCH DESIGN AND METHODS

Hyperinsulinemic-euglycemic clamps to assess insulin action in vivo. Male FOXC2 Tg and wild-type littermates weighing ~25 g (~16 weeks of age, n = 8 for each group) were housed under controlled temperature (23°C) and lighting (12 h of light, 0700–1900; 12 h of dark, 1900–0700) with free access to water and standard mouse chow. To examine the diet-induced changes in glucose metabolism, high-fat diet (55% fat by calories; Harlan Teklad, Madison, WI) was fed ad libitum for 3 weeks, and insulin action was measured. All procedures were approved by the Yale University Animal Care and Use Committee.

At least 4 days before hyperinsulinemic-euglycemic clamp experiments, whole-body fat and lean mass were measured in awake mice using ^{1}H magnetic resonance spectroscopy (Bruker Mini-spec Analyzer; Echo Medical Systems, Houston, TX) (24). Immediately following the measurement, mice were anesthetized with an intraperitoneal injection of ketamine (100 mg/kg body wt) and xylazine (10 mg/kg body wt), and an indwelling catheter was inserted in the right internal jugular vein as previously described (13). After an overnight fast, high-performance liquid chromatography–purified [3-^{3}H]glucose (0.05 μCi/min; PerkinElmer Life and Analytical Sciences, Boston, MA) was infused for 2 h (basal period) to estimate the rate of basal glucose turnover. Following the basal period, a 2-h hyperinsulinemic-euglycemic clamp experiment was conducted with a primed-continuous infusion of human insulin (15 pmol · kg^{-1} · min^{-1}, Humulin; Eli Lilly, Indianapolis, IN) to raise plasma insulin levels, while plasma glucose was maintained at basal concentrations with variable rates of 20% glucose infusion. Insulin-stimulated whole-body glucose metabolism rates were estimated with a continuous infusion of [3-^{3}H]glucose (0.1 μCi/min) during the clamps, and 2-deoxy-D-[1-^{14}C]glucose (2-[^{14}C]DG; PerkinElmer Life and Analytical Sciences) was bolus injected at 75 min of clamps to estimate the rates of insulin-stimulated tissue-specific glucose uptake as previously described (13). At the end of clamps, tissues were taken for biochemical measurements.

Biochemical assays and calculation. Plasma glucose, insulin, and fatty acid concentrations during clamps were analyzed as previously described (13). Plasma concentrations of [3-^{3}H]glucose, 2-[^{14}C]DG, and ^3H_2O were determined following deproteinization of plasma samples as previously described (13). The radioactivity of ^{3}H in tissue glycogen was determined by digesting tissue samples in potassium hydroxide and precipitating glycogen with ethanol. For the determination of tissue 2-[^{14}C]DG-6-phosphate (2-[^{14}C]DG-6-P) content, tissue samples were homogenized, and the supernatants were subjected to an ion-exchange column to separate 2-[^{14}C]DG-6-P from 2-[^{14}C]DG.

Rates of basal and insulin-stimulated whole-body glucose turnover were determined as the ratio of the [^{3}H]glucose infusion rate (dpm/min) to the specific activity of plasma glucose (dpm/μmol) at the end of the basal period and during the final 30 min of clamps, respectively. Hepatic glucose production during the hyperinsulinemic-euglycemic clamps was determined by subtracting the glucose infusion rate from the whole-body glucose uptake. Whole-body glycolysis was calculated from the rate of increase in plasma ^3H_2O concentration, determined by linear regression of the measurements at 80, 90, 100, 110, and 120 min of clamps. Whole-body glycogen plus lipid synthesis was estimated by subtracting whole-body glycolysis from whole-body glucose uptake, assuming that glycolysis and glycogen plus lipid synthesis account for the majority of insulin-stimulated glucose uptake. Glucose uptake in individual tissues was calculated from plasma 2-[^{14}C]DG profile, which was fitted with a double exponential or linear curve using MLAB (Civilized Software, Bethesda, MD) and tissue 2-[^{14}C]DG-6-P content. Skeletal muscle glycolysis and glycogen synthesis were calculated as previously described (13).

Insulin signaling analysis. Skeletal muscle samples (gastrocnemius) were obtained at the end of clamps to measure in vivo activities of insulin receptor substrate (IRS)-1–associated phosphatidylinositol (PI) 3-kinase. The activities were assessed by immunoprecipitating IRS-1 using antibodies to IRS-1 (Upstate Biotechnology, Lake Placid, NY) and assessing the incorporation of ^{32}P into PI to yield PI-3-monophosphate as previously described (13).

Measurement of intracellular fatty acyl CoA levels. To determine the intramuscular concentration of fatty acyl CoAs using liquid chromatography tandem mass spectrometry (LC/MS/MS), muscle samples (quadriceps) were homogenized and extracted as previously described (25–27). Briefly, frozen tissue samples (~100 mg) were grounded under liquid nitrogen and homogenized in 1 ml of 100 mmol/l KH_2PO_4 (pH 4.9) and 1 ml of 2-propanol. Heptadecanoyl CoA was added as internal standard. One hundred twenty-five microliters of saturated $(NH_4)_2SO_4$ and 2 ml of acetonitrile were added to the suspension then vortexed for 2 min. The emulsion was centrifuged for 10 min at 4,000 rpm, and then the supernatant was diluted with 5 ml of 100 mmol/l KH_2PO_4 (pH 4.9) for the solid-phase extraction. Before the loading, OPC (oligonucleotide purification cartridge) columns were conditioned with 5 ml of acetonitrile and 2 ml of 25 mmol/l KH_2PO_4 (pH 4.9). After loading the samples, the cartridges were washed with at least 10 ml of distilled H_2O, and then long-chain acyl CoAs were eluted slowly with 0.5 ml of 60% acetonitrile. The eluent was dried in Speedvac and finally reconstituted in 100 μl of methanol/H_2O for ESI/MS/MS analysis.

PE sciex API 3000 tandem mass spectrometer interfaced with TurboIonSpray ionization source was used for the analysis. The intracellular concentrations of long-chain fatty acyl CoAs (C16:0, C16:1, C18:0, C18:1, C18:2, and C18:3) were detected in negative electrospray mode. The doubly charged ions of these compounds were transmitted, and singly charged product ions were quantified in multiple reaction mode. Long-chain acyl CoA standards were purchased from Sigma Chemical (St. Louis, MO). The calibration of long-chain acyl CoAs showed consistent linearity from 0.2 to 20 ng/μl, and coefficient of variance was 2.1–5.5% for all long-chain acyl CoA species.

Statistical analysis. Data are expressed as means ± SE. The significance of the difference in mean values of wild-type mice fed normal chow diet (control) versus wild-type mice fed high-fat diet, FOXC2 transgenic mice fed normal chow diet, and FOXC2 transgenic mice fed high-fat diet was evaluated using the Duncan multiple range test. The statistical significance was at the $P < 0.05$ level.

RESULTS

Metabolic characteristics of FOXC2 Tg mice following high-fat diet. Despite being matched for body weight, FOXC2 Tg mice had lower whole-body fat mass but greater whole-body lean mass during regular chow diet compared with the wild-type littermates (Figs. 1*A* and *B*). Following 3 weeks of high-fat feeding, both groups equally gained total body weight. However, FOXC2 Tg mice gained significantly less whole-body fat mass but more whole-body lean mass following high-fat feeding compared with the wild-type littermates, resulting in similar total body weight (Figs. 1*A* and *B*). Overnight-fasted plasma glucose concentrations did not differ among groups during regular chow diet, whereas high-fat–fed wild-type mice showed a tendency for higher glucose levels than FOXC2 Tg mice (Table 1). Basal plasma insulin concentrations did not differ among groups during regular chow diet. In contrast, high-fat feeding significantly increased basal insulin concentrations in the wild-type mice but did not affect those of FOXC2 Tg mice (Table 1).

Hyperinsulinemic-euglycemic clamp experiments in FOXC2 Tg mice. Tissue-specific insulin action on glucose uptake and metabolism was examined during a 2-h hyperinsulinemic-euglycemic clamp in awake age-matched male wild-type and FOXC2 Tg mice following 3 weeks of high-fat feeding or regular chow diet. During the clamps, plasma insulin concentration was raised to ~350 pmol/l, while the plasma glucose concentration was maintained at ~6 mmol/l by a variable infusion of glucose in all groups (Table 1). The glucose infusion rate required to maintain euglycemia during clamps increased rapidly in the wild-type and FOXC2 Tg mice fed regular chow diet and reached a steady state within 90 min. In contrast, there was a markedly blunted insulin response during the hyperinsulinemic-euglycemic clamp studies in the wild-type

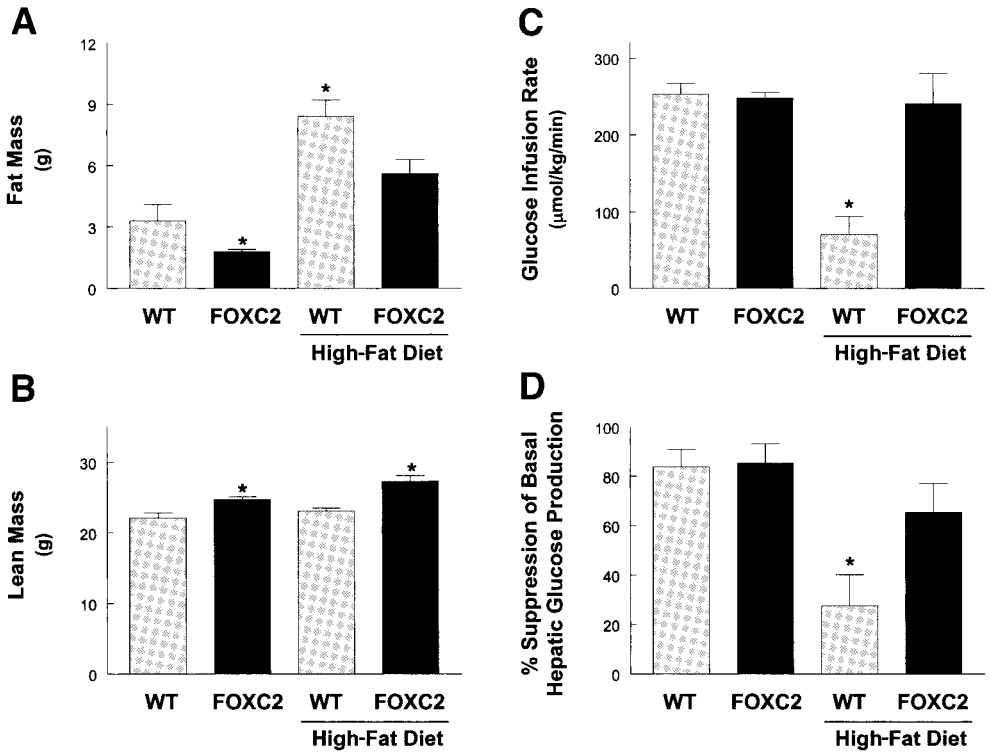

FIG. 1. Body composition and hepatic glucose production rates in the wild-type (▨) and FOXC2 Tg (■) mice with or without high-fat feeding. *A*: Whole-body fat mass. *B*: Whole-body lean mass. *C*: Steady-state glucose infusion rate obtained from averaged rates of 90–120 min of hyperinsulinemic-euglycemic clamps. *D*: Percent suppression of basal hepatic glucose production during clamps. Values are means ± SE for eight experiments. *$P < 0.05$ vs. wild-type mice.

mice after high-fat feeding, as reflected by a much lower steady-state glucose infusion rate (Fig. 1*C*). In contrast, high-fat feeding did not affect steady-state glucose infusion rate in the FOXC2 Tg mice (Fig. 1*C*). The basal hepatic glucose production rates were not different among groups (data not shown). In contrast, insulin's ability to suppress basal hepatic glucose production was severely blunted in the wild-type mice following high-fat feeding, whereas it was unaltered in the FOXC2 Tg mice (Fig. 1*D*). These findings demonstrate that FOXC2 Tg mice were protected from diet-induced insulin resistance in liver.

Insulin-stimulated whole-body glucose turnover and muscle-specific (gastrocnemius) glucose uptake were not different between wild-type mice and FOXC2 Tg mice fed regular chow diet (Figs. 2*A* and *B*). High-fat feeding decreased insulin-stimulated whole-body glucose turnover by ~40% in the wild-type mice, and this decrease was mostly accounted for by a 40% decrease in insulin-stimulated skeletal muscle glucose uptake (Figs. 2*A* and *B*). In contrast, FOXC2 Tg mice were protected from diet-induced decreases in whole-body and skeletal muscle glucose uptake (Figs. 2*A* and *B*). Insulin-stimulated whole-body glucose metabolic flux (i.e., glycolysis and glycogen plus lipid synthesis) and skeletal muscle glucose metabolic flux (i.e., glycolysis and glycogen synthesis) were not different between the wild-type and FOXC2 Tg mice fed regular chow diet (Figs. 2*C* and *D*, Figs. 3*A* and *B*). High-fat feeding significantly reduced insulin-stimulated whole-body glycolysis and glycogen plus lipid synthesis as well as skeletal muscle glycolysis in the wild-type mice (Figs. 2*C* and *D* and Fig. 3*A*). In contrast, FOXC2 Tg mice were completely protected from diet-induced decreases in whole-body and skeletal muscle glucose metabolism (Figs. 2*C* and *D* and Fig. 3*A*). These findings demonstrate that FOXC2 Tg mice were protected from diet-induced whole-body insulin resistance, and this protective effect was mostly due to their effects on skeletal muscle insulin action.

Skeletal muscle insulin signaling and fatty acyl CoA levels in FOXC2 Tg mice. Recent studies (3,28) in IRS-1 gene–disrupted mice have suggested that IRS-1 is important in insulin activation of glucose transport and glycogen synthase activity in skeletal muscle. Insulin-stimulated IRS-1–associated PI 3-kinase activity in skeletal muscle

TABLE 1
Metabolic parameters during basal and hyperinsulinemic-euglycemic clamp periods in the wild-type and FOXC2 Tg mice fed normal diet or high-fat diet for 3 weeks

			Basal period		Clamp period	
	n	Body weight (g)	Plasma glucose (mmol/l)	Plasma insulin (pmol/l)	Plasma glucose (mmol/l)	Plasma insulin (pmol/l)
Wild-type	8	26 ± 1	7.2 ± 0.4	76 ± 5	6.1 ± 0.5	339 ± 75
FOXC2 Tg	8	27 ± 1	7.0 ± 0.4	60 ± 4	6.0 ± 0.4	399 ± 75
Wild-type high-fat fed	8	32 ± 1	8.6 ± 0.9	124 ± 10*	6.3 ± 0.9	357 ± 53
FOXC2 Tg high-fat fed	8	32 ± 1	7.1 ± 0.4	82 ± 10	5.8 ± 0.5	272 ± 38

Data are means ± SE. *$P < 0.05$ vs. wild-type mice by Duncan multiple range test.

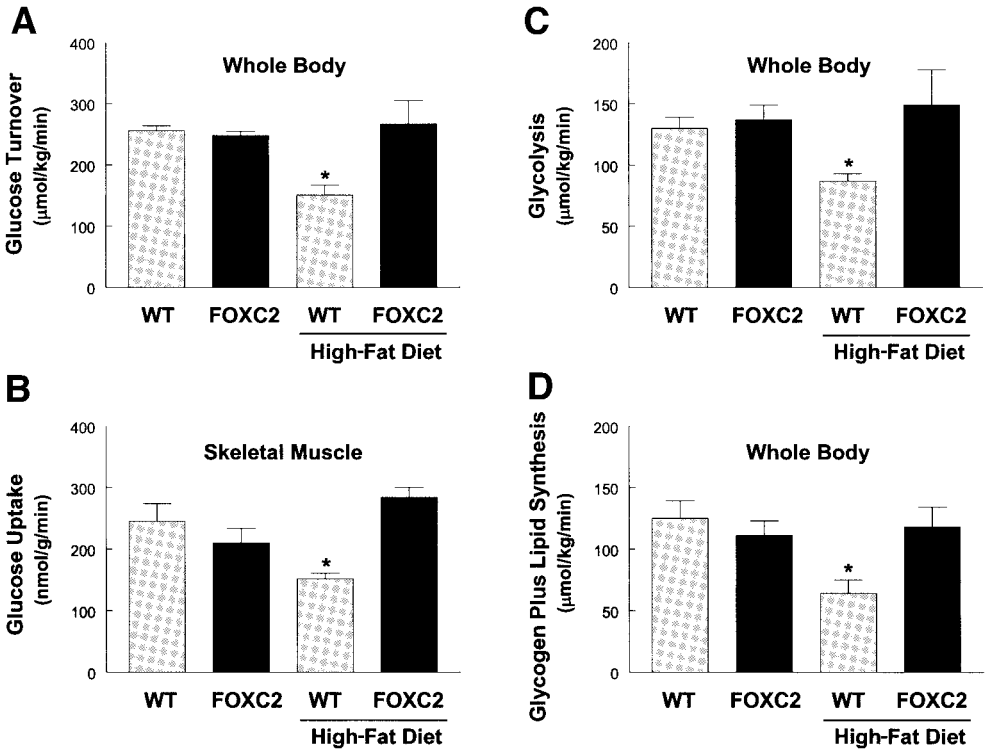

FIG. 2. Whole-body glucose metabolism and skeletal muscle glucose uptake in the wild-type (▨) and FOXC2 Tg (■) mice with or without high-fat feeding. *A*: Insulin-stimulated whole-body glucose turnover in vivo. *B*: Insulin-stimulated skeletal muscle glucose uptake in vivo. *C*: Insulin-stimulated whole-body glycolysis. *D*: Insulin-stimulated whole-body glycogen plus lipid synthesis in vivo. Values are means ± SE for eight experiments. *$P < 0.05$ vs. wild-type mice.

(gastrocnemius) was decreased by 40% in the wild-type mice following high-fat feeding (Fig. 3*C*). In contrast, FOXC2 Tg mice were protected from diet-induced defects in insulin-stimulated IRS-1–associated PI 3-kinase activity in skeletal muscle (Fig. 3*C*).

Fat-induced defects in skeletal muscle insulin action have been shown to be associated with increases in intramuscular fat and fatty acid–derived metabolites. Previous studies (17–20) have shown a strong inverse relationship between intramuscular fat content and insulin sensitivity in humans and animals. To examine whether the diet-induced changes in skeletal muscle insulin action were associated with changes in intramuscular fat contents, fatty acyl CoA concentrations were measured in skeletal muscle using LC/MS/MS. Intramuscular (quadriceps) levels of individual species and total fatty acyl CoAs (sum of C16:0, C16:1, C18:0, C18:1, C18:2, and C18:3) did not differ between the

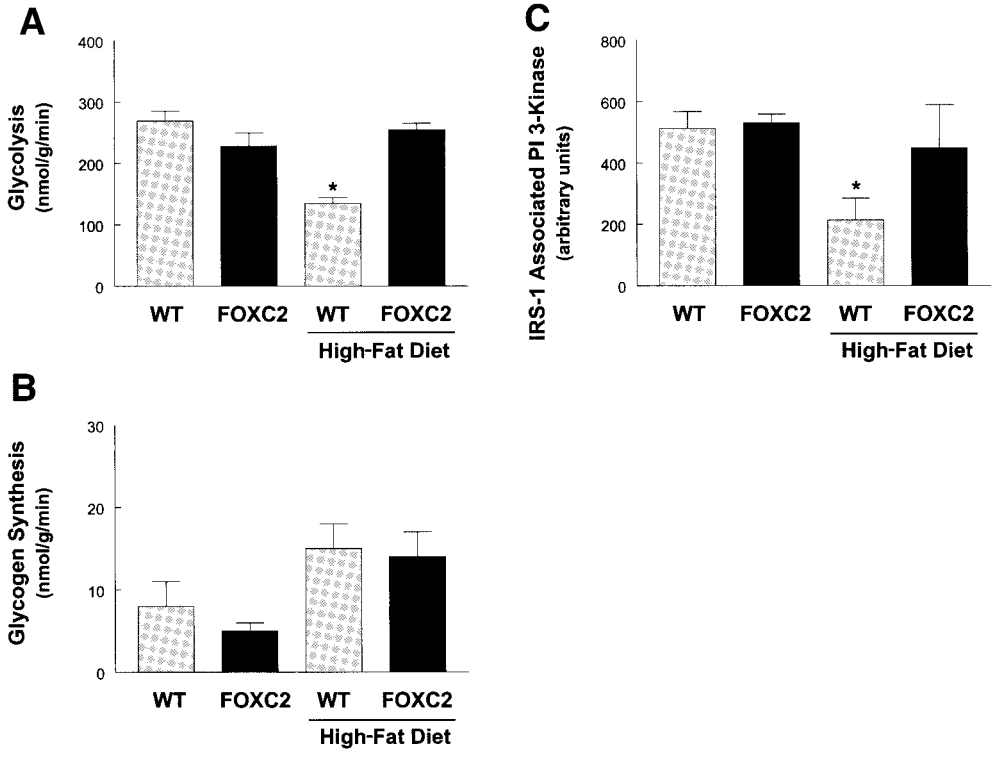

FIG. 3. Insulin-stimulated skeletal muscle glucose metabolic flux and insulin signaling in the wild-type (▨) and FOXC2 Tg (■) mice with or without high-fat feeding. *A*: Insulin-stimulated skeletal muscle glycolysis in vivo. *B*: Insulin-stimulated skeletal muscle glycogen synthesis in vivo. *C*: Insulin-stimulated IRS-1–associated PI 3-kinase activity in skeletal muscle. Values are means ± SE for eight experiments. *$P < 0.05$ vs. wild-type mice.

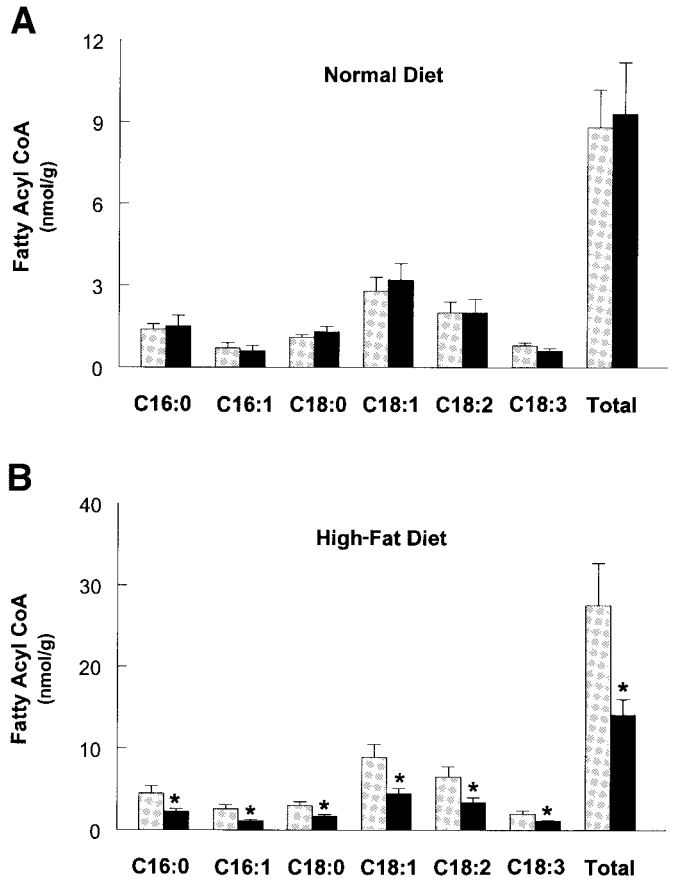

FIG. 4. Fatty acid composition of intramuscular (quadriceps) fatty acyl CoAs in the wild-type (▨) and FOXC2 Tg (■) mice fed normal diet or high-fat diet. *A*: Skeletal muscle fatty acyl CoAs in mice fed normal diet. *B*: Skeletal muscle fatty acyl CoAs in mice fed high-fat diet. Values are means ± SE for 5–8 experiments. *$P < 0.05$ vs. wild-type mice.

normal chow–fed wild-type and FOXC2 Tg mice (Fig. 4*A*). In contrast, intramuscular levels of individual species and total fatty acyl CoAs were markedly reduced in the FOXC2 Tg mice compared with the wild-type mice following high-fat feeding (Fig. 4*B*).

DISCUSSION

To determine the role of FOXC2 on tissue-specific glucose metabolism, a 2-h hyperinsulinemic-euglycemic clamp was conducted in awake FOXC2 Tg mice and wild-type littermates following 3 weeks of high-fat diet. High-fat feeding caused insulin resistance in skeletal muscle and liver of the wild-type mice, and this was associated with diet-induced defects in insulin signaling and increases in intramuscular fatty acid metabolites. In contrast, FOXC2 Tg mice were completely protected from diet-induced defects in skeletal muscle insulin signaling and action, and this was due to reduced intramuscular fatty acyl CoA levels compared with the fat-fed wild-type mice. Similarly, FOXC2 Tg mice were protected from diet-induced insulin resistance in liver. Taken together, our findings demonstrate that adipocyte-specific overexpression of FOXC2 prevented diet-induced insulin resistance in skeletal muscle and liver, and this was associated with decreases in intramuscular fatty acid metabolites. Thus, our results identify FOXC2 as potential and novel therapeutic targets in the treatment of insulin resistance and type 2 diabetes.

Our recent study has shown that fat-induced insulin resistance in skeletal muscle, using a 5-h lipid infusion, involved initial increases in intramuscular fatty acyl CoA levels and activation of protein kinase C (PKC)-θ that were subsequently followed by defects in insulin signaling and action (27). The findings of the current study support the notion that intramuscular accumulation of fatty acid metabolites (i.e., fatty acyl CoA) is the causative factor in the development of fat-induced insulin resistance. The mechanism by which increased levels of fatty acid–derived metabolites cause insulin resistance involves activation of serine kinase cascade, of which PKC-θ and/or inhibitor of κB kinase-β (IKK-β) may play a role, leading to the serine phosphorylation of IRS-1 (29–33). Recent studies (34,35) have shown that serine phosphorylation of IRS-1 prevents tyrosine phosphorylation of IRS-1 and interferes with its ability to activate PI 3-kinase, leading to insulin resistance, as occurs upon treatment with tumor necrosis factor-α and okadaic acid. In this regard, fatty acyl CoA is a potent activator of PKC-θ (36,37), while Itani et al. (30) have shown increased activity of PKC-θ in obese insulin-resistant subjects. Additionally, Yuan et al. (31) have demonstrated that activation of IKK-β resulted in defects in skeletal muscle insulin signaling, while our previous study (29) has shown that mice with heterozygous deletion of IKK-β were protected from fat-induced insulin resistance in skeletal muscle. Our present results indicate that FOXC2 Tg mice were protected from diet-induced insulin resistance in skeletal muscle and that this effect was associated with normal intramuscular fatty acyl CoA levels, which further supports this hypothesis.

Decreases in intramuscular fatty acid metabolites in the high-fat–fed FOXC2 Tg mice may be due to increased lipid metabolism in the adipose tissue of the Tg mice. We have previously shown that adipocytes of FOXC2 Tg mice expressed increased amount of mitochondria and rate of oxygen consumption (23). Elevated adipocyte metabolism also explains reduced whole-body fat mass in the FOXC2 Tg mice compared with the wild-type littermates fed regular chow diet or high-fat diet. These findings are similar to the mice lacking protein-tyrosine phosphatase (PTP)-1B, which have been shown to exhibit increased energy expenditure, low adiposity, and protection from diet-induced obesity (38). Additionally, these characteristics were associated with enhanced insulin sensitivity and skeletal muscle insulin action of the PTP-1B–null mice (38). However, increased metabolic rate of PTP-1B–null mice was mostly due to upregulation of mitochondrial biogenesis in the skeletal muscle without alteration of adipocyte metabolism or uncoupling protein expression in the PTP-1B–null mice (38). Furthermore, increased skeletal muscle insulin action of the PTP-1B–null mice was partly due to the negative regulatory role of PTP-1B on skeletal muscle insulin signaling (38). In this regard, PTPs have been shown to reduce insulin-mediated tyrosine phosphorylation of IRS-1 and IRS-1–associated PI 3-kinase activity in skeletal muscle (39–42). These effects of PTP-1B are in marked contrast to the effects of adipocyte overexpression of FOXC2 in which increased skeletal muscle insulin action was secondary to increases in adipocyte metabolism, possibly due to altered distribution of fatty acids into skeletal muscle and adipose tissue. Our

findings that intramuscular fatty acyl CoA levels did not significantly increase despite high-fat feeding, contrary to the significant increase in the fat-fed wild-type mice, further implicate the scenario in which fatty acids were largely metabolized by adipose tissue, which in turn prevented their accumulation in skeletal muscle of the FOXC2 Tg mice. Interestingly, whole-body lean mass was increased in the FOXC2 Tg mice fed regular chow diet or high-fat diet at a level similar to decreases in fat mass resulting in comparable total body weight to the wild-type mice. It is unclear how alteration in adipocyte metabolism and/or whole-body insulin sensitivity caused changes in whole-body lean mass of the FOXC2 Tg mice.

The mechanism by which fatty acids were distributed to adipose tissue may involve increased adipocyte expression of perixisome proliferator–activated receptor (PPAR)-γ in the FOXC2 Tg mice (23,43–45). Our recent study has shown that a treatment of PPAR-γ agonist, rosiglitazone, ameliorated insulin resistance in skeletal muscle of the A-ZIP/F-1 lipodystrophic mice by increasing distribution of fatty acids to liver and away from skeletal muscle (46), and this was associated with increased hepatic expression of PPAR-γ in the rosiglitazone-treated lipodystrophic mice (47). Thus, this finding is consistent with our observation that adipocyte-specific overexpression of FOXC2 increased adipocyte expression of PPAR-γ, caused redistribution of fatty acids, and prevented diet-induced accumulation of fatty acyl CoA and insulin resistance in the skeletal muscle (48,49). Furthermore, FOXC2 Tg mice were also protected from diet-induced insulin resistance in liver, and a similar mechanism involving altered distribution of fatty acids may also be responsible for the liver phenotype.

Alteration in adipocyte metabolism has also been shown to regulate whole-body glucose homeostasis in the mice with adipocyte-specific deletion of insulin receptor (FIRKO; 50). Bluher et al. (50) have recently demonstrated that FIRKO mice exhibited reduced whole-body fat mass and protection from diet-induced obesity as well as insulin resistance. These metabolic effects were associated with increased expression of lipid metabolism genes (e.g., fatty acid synthase) in the adipocytes of FIRKO mice (48). Interestingly, FIRKO mice also exhibited a polarization in adipocyte size in which the range of cell size shifted in favor of smaller adipocyte size than large adipocyte size compared with the wild-type mice (50). Whether such polarization in adipocyte size also occurs in FOXC2 Tg mice and is associated with altered adipocyte metabolism is unknown. Thus, our results indicate indirect effects of adipocyte-specific overexpression of FOXC2 on skeletal muscle and liver glucose metabolism and that such effects most likely stem from enhanced lipid oxidation in white and/or brown adipose tissues (23). Alternatively, altered expression of adipocyte-derived circulating factors (e.g., leptin, adiponectin, resistin), which have recently been shown to play a role in skeletal muscle insulin resistance (51–54), may explain some of our findings in the FOXC2 Tg mice.

Overall, our findings demonstrated that FOXC2 Tg mice were protected from diet-induced insulin resistance in skeletal muscle and liver, which was partly due to altered distribution of fatty acids. Altered partitioning of fatty acids was most likely due to increased adipocyte expression of genes associated with metabolism in the FOXC2 Tg mice. Thus, altering the white adipocyte phenotype and gene expression pattern toward those of brown adipocytes (23) may induce favorable metabolic adaptations as reported here. Taken together, our results identify FOXC2 as a novel therapeutic target for the treatment of obesity and obesity-associated type 2 diabetes.

ACKNOWLEDGMENTS

This study was conducted at the Yale Mouse Metabolic Phenotyping Center and supported by grants from the U.S. Public Health Service (U24 DK-59635 to G.I.S. and J.K.K., R01 DK-40936 to G.I.S., and P30 DK-45735 to G.I.S.). This study was also supported by the grant from the American Diabetes Association (7-01-JF-05 to J.K.K.). This work was further made possible with support from The Swedish Research Council (K2002-99BI-14383-01A to S.E. and K2002-31X-12186-06A to S.E.), EU Grants (QLK3-CT-2002-02149 to S.E. and LSHM-CT-2003-503041 to S.E.), The Arne and IngaBritt Lundberg Foundation, and The Söderberg Foundation.

G.I.S. is an investigator of the Howard Hughes Medical Institute. We are grateful to Aida Groszmann for technical assistance.

REFERENCES

1. Shaw JE, Zimmet PZ, McCarty D, de Courten M: Type 2 diabetes worldwide according to the new classification and criteria. *Diabetes Care* 23 (Suppl. 2):B5–B10, 2000
2. Kahn CR: Insulin action, diabetogenes, and the cause of type II diabetes. *Diabetes* 43:1066–1084, 1994
3. DeFronzo RA: The triumvirate: beta-cell, muscle, liver. A collusion responsible for NIDDM. *Diabetes* 37:667–687, 1988
4. McGarry JD: What if Minkowski had been ageusic? An alternative angle on diabetes. *Science* 258:766–770, 1992
5. Boden G: Obesity, free fatty acids, and insulin resistance. *Cur Opin In Endo & Diabetes* 8:235–239, 2001
6. Kraegen EW, James DE, Storlien LH, Burleigh KM, Chisholm DJ: In vivo insulin resistance in individual peripheral tissues of the high fat fed rat: assessment by euglycaemic clamp plus deoxyglucose administration. *Diabetologia* 29:192–198, 1986
7. Petersen KF, Oral EA, Dufour S, Befroy D, Ariyan C, Yu C, Cline GW, DePaoli AM, Taylor SI, Gorden P, Shulman GI: Leptin reverses insulin resistance and hepatic steatosis in patients with severe lipodystrophy. *J Clin Invest* 109:1345–1350, 2002
8. Hotamisligil GS, Shargill NS, Spiegelman BM: Adipose expression of tumor necrosis factor-alpha: direct role in obesity-linked insulin resistance. *Science* 259:87–91, 1993
9. Steppan CM, Bailey ST, Bhat S, Brown EJ, Banerjee RR, Wright CM, Patel HR, Ahima RS, Lazar MA: The hormone resistin links obesity to diabetes. *Nature* 409:307–312, 2001
10. Yamauchi T, Kamon J, Waki H, Terauchi Y, Kubota N, Hara K, Mori Y, Ide T, Murakami K, Tsuboyama-Kasaoka N: The fat-derived hormone adiponectin reverses insulin resistance associated with both lipoatrophy and obesity. *Nat Med* 7:941–946, 2001
11. Hotta K, Funahashi T, Arita Y, Takahashi M, Matsuda M, Okamoto Y, Iwahashi H, Kuriyama H, Ouchi N, Maeda K, Nishida M, Kihara S, Sakai N, Nakajima T, Hasegawa K, Muraguchi M, Ohmoto Y, Nakamura T, Yamashita S, Hanafusa T, Matsuzawa Y: Plasma concentrations of a novel, adipose-specific protein, adiponectin, in type 2 diabetic patients. *Arterioscler Thromb Vasc Biol* 20:1595–1599, 2000
12. Kahn CR, Chen L, Cohen SE: Unraveling the mechanism of action of thiazolidinediones. *J Clin Invest* 106:1305–1307, 2000
13. Kim H-J, Higashimori T, Park S-Y, Choi H, Dong J, Kim Y-J, Noh H-L, Cho Y-R, Cline G, Kim Y-B, Kim JK: Differential effects of interleukin-6 and -10 on skeletal muscle and liver insulin action in vivo. *Diabetes* 53:1060–1067, 2004
14. Reaven GM: Role of insulin resistance in human disease. *Diabetes* 37:1595–1607, 1988

15. Shulman GI: Cellular mechanisms of insulin resistance. *J Clin Invest* 106:171–176, 2000
16. Kraegen EW, Cooney GJ, Ye J, Thompson AL: Triglycerides, fatty acids and insulin resistance: hyperinsulinemia. *Exp Clin Endocrinol Diabetes* 109: S516–S526, 2001
17. Boden G, Lebed B, Schatz M, Homko C, Lemieux S: Effects of acute changes of plasma free fatty acids on intramyocellular fat content and insulin resistance in healthy subjects. *Diabetes* 50:1612–1617, 2001
18. Kim JK, Fillmore JJ, Chen Y, Yu C, Moore IK, Pypaert M, Lutz EP, Kako Y, Velez-Carrasco W, Goldberg IJ, Breslow JL, Shulman GI: Tissue-specific overexpression of lipoprotein lipase causes tissue-specific insulin resistance. *Proc Natl Acad Sci U S A* 98:7522–7527, 2001
19. Krssak M, Falk Petersen K, Dresner A, DiPietro L, Vogel SM, Rothman DL, Roden M, Shulman GI: Intramyocellular lipid concentrations are correlated with insulin sensitivity in humans: a ^{1}H NMR spectroscopy study. *Diabetologia* 42:113–116, 1999
20. Perseghin G, Scifo P, De Cobelli F, Pagliato E, Battezzati A, Arcelloni C, Vanzulli A, Testolin G, Pozza G, Del Maschio A: Intramyocellular triglyceride content is a determinant of in vivo insulin resistance in humans: a ^{1}H-^{13}C nuclear magnetic resonance spectroscopy assessment in offspring of type 2 diabetic patients. *Diabetes* 48:1600–1606, 1999
21. Hajri T, Han XX, Bonen A, Abumrad NA: Defective fatty acid uptake modulates insulin responsiveness and metabolic responses to diet in CD36-null mice. *J Clin Invest* 109:1381–1389, 2002
22. Kim JK, Gimeno RE, Higashimori T, Kim H-J, Choi H, Punreddy S, Mozell RL, Tan G, Stricker-Krongrad A, Hirsch DJ, Fillmore JJ, Liu Z-X, Dong J, Cline G, Stahl A, Lodish HF, Shulman GI: Inactivation of fatty acid transport protein 1 prevents fat-induced insulin resistance in skeletal muscle. *J Clin Invest* 113:756–763, 2001
23. Cederberg A, Gronning LM, Ahren B, Tasken K, Carlsson P, Enerback S: FOXC2 is a winged helix gene that counteracts obesity, hypertriglyceridemia, and diet-induced insulin resistance. *Cell* 106:563–573, 2001
24. Tinsley FC, Taicher GZ, Heiman ML: Evaluation of a quantitative magnetic resonance method for mouse whole body composition analysis. *Obesity Res* 12:150–160, 2004
25. Bligh EG, Dyer WJ: A rapid method of total lipid extraction and purification. *Can J Biochem Physiol* 37:911–917, 1959
26. Deutsch J, Grange E, Rapoport SI, Purdon AD: Isolation and quantitation of long-chain acyl-coenzyme A esters in brain tissue by solid-phase extraction. *Anal Biochem* 220:321–323, 1994
27. Yu C, Chen Y, Cline GW, Zhang D, Zong H, Wang Y, Bergeron R, Kim JK, Cushman SW, Cooney GJ, Atcheson B, White MF, Kraegen EW, Shulman GI: Mechanism by which fatty acids inhibit insulin activation of insulin receptor substrate-1 (IRS-1)-associated phosphatidylinositol 3-kinase activity in muscle. *J Biol Chem* 277:50230–50236, 2002
28. Previs SF, Withers DJ, Ren J-M, White MF, Shulman GI: Contrasting effects of IRS-1 *versus* IRS-2 gene disruption on carbohydrate and lipid metabolism in vivo. *J Biol Chem* 275:38990–38994, 2000
29. Kim JK, Kim Y-J, Fillmore JJ, Chen Y, Moore I, Lee J, Yuan M, Li ZW, Karin M, Perret P, Shoelson SE, Shulman GI: Prevention of fat-induced insulin resistance by salicylate. *J Clin Invest* 108:437–446, 2001
30. Itani SI, Zhou Q, Pories WJ, MacDonald KG, Dohm GL: Involvement of protein kinase C in human skeletal muscle insulin resistance and obesity. *Diabetes* 49:1353–1358, 2000
31. Yuan M, Konstantopoulos N, Lee J, Hansen L, Li ZW, Karin M, Shoelson SE: Reversal of obesity- and diet-induced insulin resistance with salicylates or targeted disruption of IKK-beta. *Science* 293:1673–1677, 2001
32. Schmitz-Peiffer C, Browne CL, Oakes ND, Watkinson A, Chisholm DJ, Kraegen EW, Biden TJ: Alterations in the expression and cellular localization of protein kinase C isozymes epsilon and theta are associated with insulin resistance in skeletal muscle of the high-fat-fed rats. *Diabetes* 46:169–178, 1997
33. Kim JK, Fillmore JJ, Sunshine MJ, Albrecht B, Higashimori T, Kim D-W, Liu Z-X, Soos TJ, Cline GW, O'Brien WR, Littman DR, Shulman GI: PKC-theta knockout mice are protected from fat-induced insulin resistance. *J Clin Invest* 114:823–827, 2004
34. Rui L, Yuan M, Frantz D, Shoelson S, White MF: SOCS-1 and SOCS-3 block insulin signaling by ubiquitin-mediated degradation of IRS1 and IRS2. *J Biol Chem* 277:42394–42398, 2002
35. Pederson TM, Kramer DL, Rondinone CM: Serine/threonine phosphorylation of IRS-1 triggers its degradation: possible regulation by tyrosine phosphorylation. *Diabetes* 50:24–31, 2001
36. Griffin ME, Marcucci MJ, Cline GW, Bell K, Barucci N, Lee D, Goodyear LJ, Kraegen EW, White MF, Shulman GI: Free fatty acid-induced insulin resistance is associated with activation of protein kinase C θ and alterations in the insulin signaling cascade. *Diabetes* 48:1270–1274, 1999
37. Chalkley SM, Hettiarachchi M, Chisholm DJ, Kraegen EW: Five-hour fatty acid elevation increases muscle lipids and impairs glycogen synthesis in the rat. *Metabolism* 47:1121–1126, 1998
38. Klaman LD, Boss O, Peroni OD, Kim JK, Martino JL, Zabolotny JM, Moghal N, Lubkin M, Kim YB, Sharpe AH, Stricker-Krongrad A, Shulman GI, Neel BG, Kahn BB: Increased energy expenditure, decreased adiposity, and tissue-specific insulin sensitivity in protein-tyrosine phosphatase 1B-deficient mice. *Mol & Cell Biology* 20:5479–5489, 2000
39. Ahamd F, Azevedo JL, Cortright R, Dohm GL, Goldstein BJ: Alterations in skeletal muscle protein-tyrosine phosphatase activity and expression in insulin-resistant human obesity and diabetes. *J Clin Invest* 100:449–458, 1997
40. Hashimoto N, Feener EP, Zhang WR, Goldstein BJ: Insulin receptor protein-tyrosine phosphatases: leukocyte common antigen-related phosphatase rapidly deactivates the insulin receptor kinase by preferential dephosphorylation of the receptor regulatory domain. *J Biol Chem* 267: 13811–13814, 1992
41. Kenner KA, Anyanwu E, Olefsky JM, Kusari J: Protein-tyrosine phosphatase 1B is a negative regulator of insulin- and insulin-like growth factor-I-stimulated signaling. *J Biol Chem* 271:19810–19819, 1996
42. Ren JM, Li PM, Zhang WR, Sweet LJ, Cline G, Shulman GI, Livingston JN, Goldstein BJ: Transgenic mice deficient in the LAR protein-tyrosine phosphatase exhibit profound defects in glucose homeostasis. *Diabetes* 47:493–497, 1998
43. Saltiel AR, Olefsky JM: Thiazolidinediones in the treatment of insulin resistance and type II diabetes. *Diabetes* 45:1661–1669, 1996
44. Lehmann JM, Moore LB, Smith-Oliver TA, Wilkison WO, Wilson TM, Kliewer SA: An antidiabetic thiazolidinedione is a high affinity ligand for peroxisome proliferators-activated receptor gamma (PPAR gamma). *J Biol Chem* 270:12953–12956, 1995
45. Mayerson AB, Hundal RS, Dufour S, Lebon V, Befroy D, Cline GW, Enocksson S, Inzucchi SE, Shulman GI, Petersen KF: The effects of rosiglitazone on insulin sensitivity, lipolysis, and hepatic and skeletal muscle triglyceride content in patients with type 2 diabetes. *Diabetes* 51:797–802, 2002
46. Kim JK, Fillmore JJ, Gavrilova O, Chao L, Higashimori T, Choi H, Kim H-J, Yu C, Chen Y, Qu X, Haluzik M, Reitman ML, Shulman GI: Differential effects of rosiglitazone on skeletal muscle and liver insulin resistance in A-ZIP/F-1 fatless mice. *Diabetes* 52:1311–1318, 2003
47. Chao L, Marcus-Samuels B, Mason MM, Moitra J, Vinson C, Arioglu E, Gavrilova O, Reitman ML: Adipose tissue is required for the antidiabetic, but not for the hypolipidemic, effect of thiazolidinediones. *J Clin Invest* 106:1221–1228, 2000
48. Lapsys NM, Kriketos AD, Lim-Fraser M, Poynten AM, Lowy A, Furler SM, Chisholm DJ, Cooney GJ: Expression of genes involved in lipid metabolism correlate with peroxisome proliferator-activated receptor γ expression in human skeletal muscle. *J Clin Endocrinol Metab* 85:4293–4297, 2000
49. Loviscach M, Rehman N, Carter L, Mudaliar S, Mohadeen P, Ciaraldi TP, Veerkamp JH, Henry RR: Distribution of peroxisome proliferator-activated receptors (PPARs) in human skeletal muscle and adipose tissue: relation to insulin action. *Diabetologia* 43:304–311, 2000
50. Bluher M, Michael OD, Peroni OD, Ueki K, Carter N, Kahn BB, Kahn CR: Adipose tissue selective insulin receptor knockout protects against obesity and obesity-related glucose intolerance. *Dev Cell* 3:25–38, 2002
51. Nagaev I, Smith U: Insulin resistance and type 2 diabetes are not related to resistin expression in human fat cells or skeletal muscle. *Biochem Biophys Res Comm* 285:561–564, 2001
52. Sentinelli F, Romeo S, Arca M, Filippi E, Leonetti F, Banchieri M, DiMario U, Baroni MG: Human resistin gene, obesity, and type 2 diabetes: mutation analysis and population study. *Diabetes* 51:860–862, 2002
53. Arita Y, Kihara S, Ouchi N, Takahashi M, Maeda K, Miyagawa J, Hotta K, Shimomura I, Nakamura T, Miyaoka K, Kuriyama H, Nishida M, Yamashita S, Okubo K, Matsubara K, Muraguchi M, Ohmoto Y, Funahashi T, Matsuzawa Y: Paradoxical decrease of an adipose-specific protein, adiponectin, in obesity. *Biochem Biophys Res Commun* 257:79–83, 1999
54. Hotta K, Funahashi T, Bodkin NL, Ortmeyer HK, Arita Y, Hansen BC, Matsuzawa Y: Circulating concentrations of adipocyte protein adiponectin are decreased in parallel with reduced insulin sensitivity during the progression to type 2 diabetes in rhesus monkeys. *Diabetes* 50:1126–1133, 2001